Chalcogenide Letters Vol. 5, No. 10, October 2008, p. 229-237

STUDY OF THERMAL PARAMETERS OF $Sn_{10}Sb_{20}Se_{70-X}Te_X$ ($0 \leq X \leq 12$) CHALCOGENIDE GLASSES

Ravi Chander*, R. Thangaraj
Semiconductor Laboratory, Department of Applied Physics, Guru Nanak Dev University, Amritsar 143005, India

Thermal studies of $Sn_{10}Sb_{20}Se_{70-X}Te_X$ ($0 \leq X \leq 12$) have been performed using Differential scanning calorimetery (DSC) at different heating rates. Glass transition temperature and crystallization temperature were evaluated from DSC scans and are found to increase with heating rate. The glass transition temperature T_g increases with increase in Te contents upto X=10 and then decreases for X=12 while the crystallization temperature T_p increases upto X=4 and then decreases with further substitution of Te. The apparent activation energy for glass transition and activation energy for crystallization were calculated using Kissinger, modified Kissinger and Matusita equations. The difference in the bond energies of Se and Te with Sn and Sb leads to decrease of T_g initially but increases with further substitution of Te. The parameters for glass stability reflects X= 4 composition as best glass stabilty among the composition studied.

(Received September 23, 2008; accepted September 29, 2008)

Keywords: Sn-Sb-Se-Te; Chalcogenide glasses; Thermal properties

1. Introduction

Recently chalcogenide materials are widely studied for their potenial applications in active as well as passive solid-state electronics and optical devices. The applications include photoreceptor in xerography [1], optical recording and memory switching [2, 3], infrared optical fibres and waveguides [4] and non-linear optics [5]. Due to high transmittance in the IR region of chalcogenide glasses, these materials are being used as an active as well as passive component in IR optical devices. The chalcogenide materials containing S, Se and Te have high transmittance in the 0.8-7, 1-10, and 2-12 μm, respectively [8]. Chalcogenide glasses with heavy atomic mass elements show small glass forming region but on the other hand has advantage of having higher transmittance in IR region due to reduction in optical band gap and thus low optical losses [2]. This technological advantage increases the interest in the chalcogenide systems having Sn, Sb as heavy elements.The optical and electrical properties of these materials are significantly modified by substitution or addition of impurity elements in the chalcogenide system.

P Kuamr *et al.* [10] showed the glassy nature of the $Sn_xSb_{20}Se_{80-x}$ ($8 \leq X \leq 18$) and showed that the system with X=10 with average coordination number Z=2.40 is the best glass former. The aim of the present work is to find out the effect of isoelectronic substitution of chalcogen element Te with Se on thermal and electrical properties of the glassy $Sn_{10}Sb_{20}Se_{70}$ system [10]. There have been reports of Se-Te system having better corrosion resistance [9], which makes it a prospective material for phase change memory application. The study of crystallization kinetics of amorphous materials has been widely discussed in literature [6,7],[11]. Different techniques viz isothermal and non-isothermal are employed to study the crystallization kinetics in solids. In isothermal technique, the temperature is quickly increased to above T_g and heat evolved is analyzed. On the other hand, in case of non-isothermal technique, the sample is heated at constant heating rate and heat evolved is analyzed. non-isothermal technique employs the use of

* Corresponding author: rcohri@gmail.com

differential scanning calorimetery. There have been many theoretical models developed to explain the crystallization kinetics [14-16], [22]. In the present work, these models are used to calculate the apparent activation energy for glass transition and activation energy for crystallization.

2. Experimental Procedure

Bulk samples of $Sn_{10}Sb_{20}Se_{70-X}Te_X$ ($0 \leq X \leq 12$) were prepared using conventional melt quenching techinque. The quartz tubes of 5mm outer diameter and ~10 cm length were sealed from one end and were rinsed using organic solvant (acetone). These tubes (ampoules) were cleaned with aqua regia and finally with HF for two hours each and then dried. The appropriate amounts of constituent elements of 4N purity were weighed and sealed in the cleaned ampoules under vacuum sealing at ~ 10^{-5} mbar. The sealed ampoules were heated in furnance at 5 K/min heating rate upto 1123K and were kept for 48 hours.The ampoules were frequently rocked to ensure homogenous mixing of constituents. The ampoules were then quenched in ice cold water to obtain amorphous materials. The quenched ampoules were etched in 60% V/V HF + 40% V/V H_2O_2 for 40-48 hours for extracting the materials. The bulk material extracted was ground finely and used for X-ray diffraction (XRD) and differential scanning calorimetry (DSC) studies. XRD studies were done using Phillips PAN ANALYTICAL machine and X-Ray of Cu $K_{\square}$ line to check the amorphous nature of the materials. DSC studies were done using Mettler Toledo Star^e system from RT- 773K at different heating rates viz (5,10,15 and 20 K/min) under N_2 environment and empty reference pan. The glass transition temperature is defined as the temperature corresponding to the intersection of two linear portions adjoining the transitions elbow of the DSC trace in the endothermic direction. The onset crystallization temperature T_c, has been defined as the temperature corresponding to the intersection of the two linear portions adjoining the transition elbow of the DSC trace in the exothermic direction. The fraction X_c crystallized at a temperature T was calculated using the relation $X_c = A_T/A$ where A is the total area of the exotherm between Tc and the temperature at which crystallization is completed, A_T is the area between onset temperature Tc and temperature T.

3. Results and disscussion

Powder of bulk samples was used to check the amorphous nature of the material using XRD technique. Fig 1 shows the XRD pattern of the samples. XRD patterns are shifted on intensity scale for clear visiblity. Absence of any sharp peak indicates the amorphous nature of these samples.

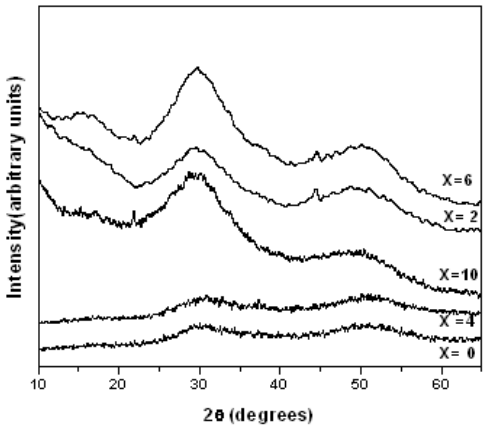

Fig. 1. XRD pattern of $Sn_{10}Sb_{20}Se_{70-X}Te_X$ glasses. The absence of any sharp peak in the pattern shows the amorphous nature of the materials.

Fig 2 shows the typical DSC plot of sample having X = 6. Samples with other X values show similar plots.

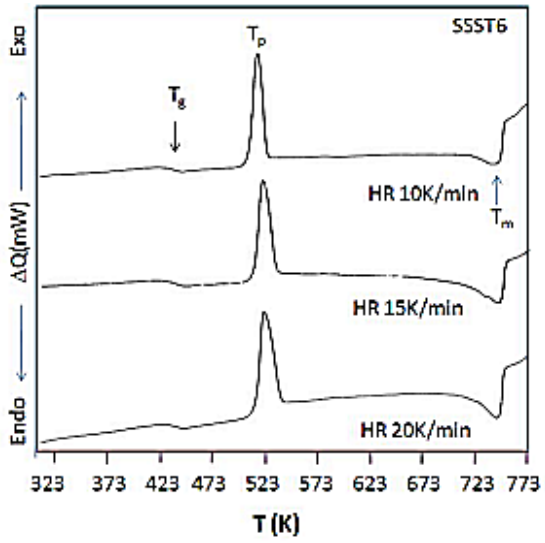

Fig. 2. DSC Plot of $Sn_{10}Sb_{20}Se_{64}Te_6$ at different heating rates. The glass transition, Peak Crystallization and melting temperature are marked in plot.

3.1 Glass Transition

The glass transition temperature T_g as obtained from the DSC plots shows a monotonic increase upto X=10 and then decreases as shown in fig 3.

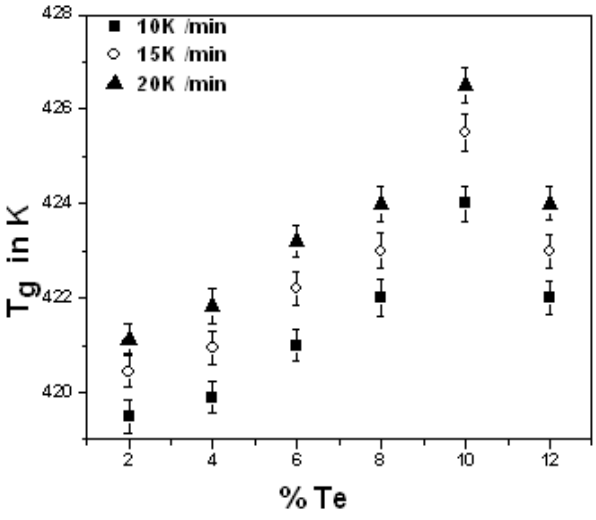

Fig. 3. Variation of T_g with Tellurium contents in the samples.

The value of T_g shows a shift towards higher temperature with increase in heating rate, α as shown in fig 4 for $Sn_{10}Sb_{20}Se_{68}Te_2$ sample.

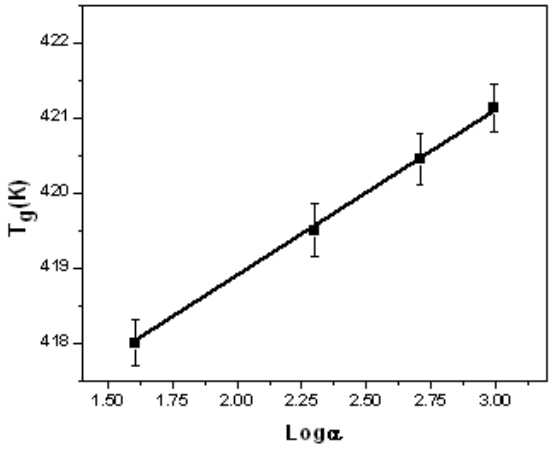

Fig. 4. Plot of linear Variation of T_g with heating rate α for $Sn_{10}Sb_{20}Se_{68}Te_2$ sample.

The empirical realtion for glass transition variation with heating rate

$$T_g = A + B \log\alpha \quad (1)$$

Where, A and B are constants holds good for all samples. The variation of B values from 2.35 to 3.60 reveals the structural changes occuring in the sample as the composition is varied [12]. The apparent activation energy for glass transition was calculated using Kissinger equation [13].

$$\ln(T_g^2/\alpha) + \text{constant} = E_{gl}/ RT_g \quad (2)$$

Where α, R and E_{gl} are heating rate, gas constant and apparent activation energy for glass transition respectively. The slope of ln (T_g^2/α) versus $1000/T_g$ plot gives the value of E_{gl} as shown in fig 5. The apparent activation energy for glass transition shows a decreasing trend with increasing tellurium contents.

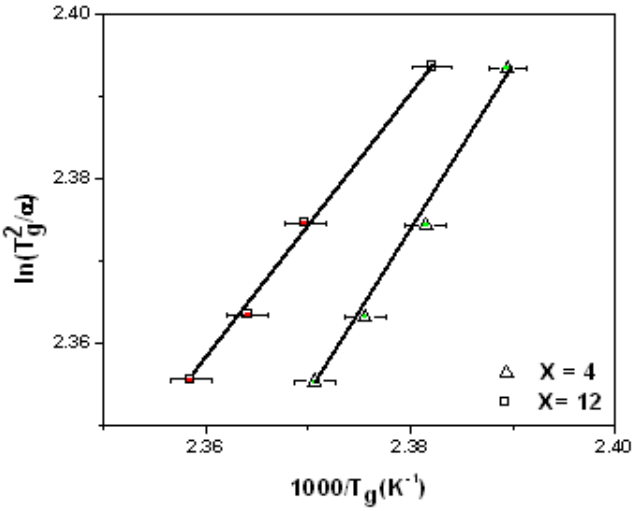

Fig. 5. Plot of ln (T_g^2/α) versus $1000/T_g$ for samples $Sn_{10}Sb_{20}Se_{70-X}Te_X$ with X=4 and 12.

3.2 Crystallization

The activation energy for crystallization was calculated from the modified Kissinger equation [14]

$$\ln(\alpha^n / T_p^2) = -mE_c / RT_p + \ln K' \quad (3)$$

Where K' is the constant containing factors representing the thermal history of the sample. The n and m are factors having values between 1 and 4 depending upon the morphology of the growth.The slope of lnα versus $1000/T_p$ gives the value of mE_c/n as shown in fig 6.

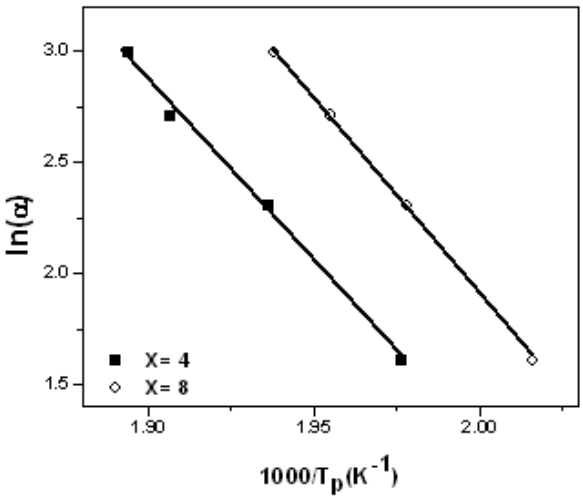

Fig. 6. Plot of ln α with $1000/T_p$ for X=4 and 8.

In case of non-isothermal crystallization the activation energy can be calculated using the Matusita equation [15]

$$\ln\{-\ln(1-X_c)\} = -n\ln\alpha - 1.052mE_c/RT_p \quad (4)$$

Where X_c is the volume fraction of crystals precipitated in the glass heated at uniform heating rate α, E_c is the crystallization activation energy, T_p is the peak crystallization Temperature and n and m are constants representing morphology of the growth. Mahadevan *et al* [16] has shown that n can take value 4,3,2,1 related to different types of glass crystal transformation mechanism. n=4 represents volume nucleation and three dimensional growth, n=3 represent volume nucleation and two dimensional growth, n=2 represents volume nucleation and one dimensional growth, n=1 represents surface nucleation and one dimensional growth from surface to inside. The value of n can be calculated from the slop of the straight line of plot of ln [-ln (1-X_c)] versus lnα at constant temperature. Fig 7 shows the plot of ln [-ln (1-X_c)] versus ln σ at two different temperature for $Sn_{10}Sb_{20}Se_{64}Te_6$ sample.the value of n comes out to be 4.15-4.51. Since the sample were not given any heat treatment before DSC experiments thus value of m can be taken as n-1 i.e. 3. Thus in the case of our samples, values of n=4 and m=3 reveal volume nucleation and three dimensional growth.

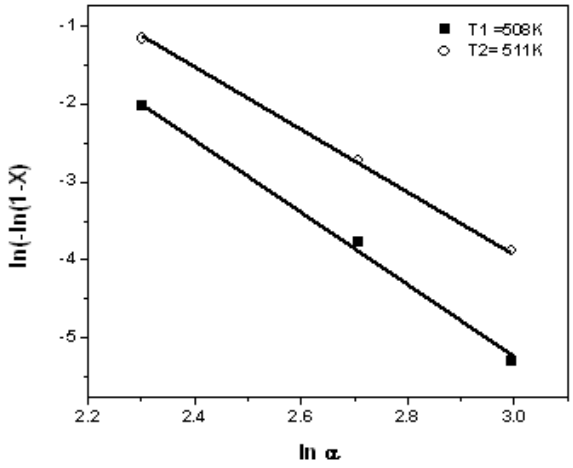

Fig.7. Plot of ln [-ln (1-Xc)] and ln α at two different temperatures for $Sn_{10}Sb_{20}Se_{64}Te_6$ sample.

Fig 8 shows the variation of fraction crystallized with temperature.and shows an increase of the fraction crystallized as the temperature is increased during heating up of the sample in DSC runs.

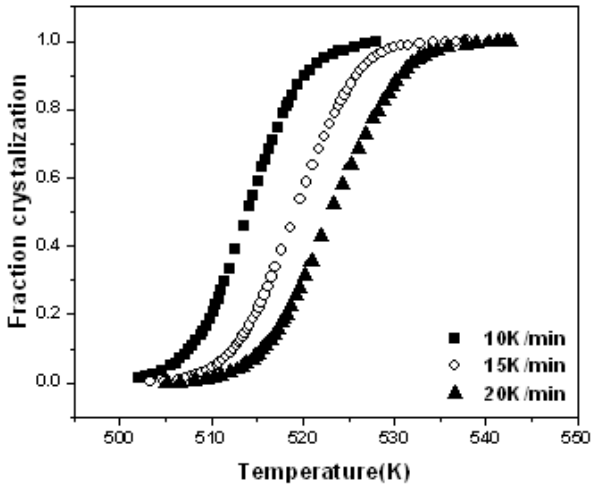

Fig.8. Shows the increase of fraction crystallization as the temperature increases with heating of the sample.

Fig 9 shows the plot of ln[-ln(1-X_c)] with 1000/Tp at different heating rates for $Sn_{10}Sb_{20}Se_{64}Te_6$ sample. From the slope of the straight line drawn, one can evaluate the value of mE_c. The deviation from the straight line nature at higher temperature is due to saturation of nucleation sites during the latter stage in the process of crystallization [17].

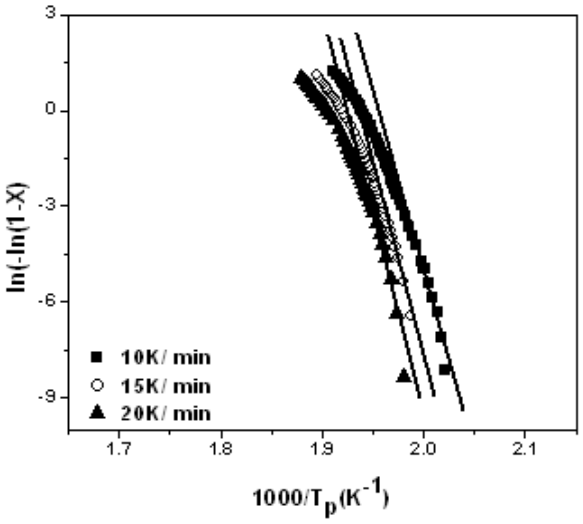

Fig. 9. Plot of ln [-ln (1-Xc)] versus 1000/T_p.

Using the value of n and m, the activation energy of crystallization was calculated for both modified Kissinger and Matusita methods. The calculated values of E_c are given in Table 1 as E_c (MK) and E_c (ME) for modified Kissinger equation and Matusita equation respectively.

Table 1 value of B, E_{gl}, n, m, E_c (MK), E_c (ME).

% Te	B	E_{gl} (Kcalmol^{-1})	mE_c/n (MK) (Kcalmol^{-1})	n	m	E_c (MK) (Kcalmol^{-1})	mE_c(ME) (Kcalmol^{-1})	E_c (ME) (Kcalmol^{-1})
2	2.35	73.81	20.53	4.31	3	29.50	88.65	29.55
4	2.51	71.29	20.01	4.51	3	30.08	129.50	43.16
6	3.20	56.37	21.19	4.23	3	29.87	107.22	35.74
8	3.00	60.44	17.54	4.28	3	25.02	121.95	40.65
10	3.60	50.74	18.83	4.15	3	26.04	115	38.33
12	3.00	61.77	20.74	4.33	3	29.93	106.5	35.5

3.3 Glass stability

Different simple quantitative methods have been suggested for evaluating the stability of glasses [18] [19] [20] [21] using the parameters of glass transition temperature T_g, onset of crystallization temperature T_c, peak crystallization temperature T_p and melting temperature T_m obtained from the DSC data. Sakka and Meckenzie [21] used the ratio of $T_{rg} = T_g / T_m$ as glass stability parameter. Dietzel [18] introduced the glass criterion $\Delta T = T_g - T_c$ which is often an important parameter to reflect the thermal stability of the glasses. Hruby [19] introduced the parameter $H_r = \Delta T/(T_m - T_p)$. Saad and Poulain introduced the two weighted parameters H' and S,

$H' = \Delta T / T_g$ and $S = (T_p - T_c)\Delta T / T_g$ respectively. The values of these parameters are given in Table 2.

Table 2 various thermal stability parameters.

Composition	T_g	T_c	T_p	T_m	H_r	H'	S	T_{rg}
2	419.5	499	508	739	0.34416	0.18951	1.7056	0.56766
4	419.9	503	516.5	742	0.36851	0.1979	2.67171	0.5659
6	421	54.75	513.3	743	0.36461	0.19893	1.70086	0.56662
8	422	501.21	505.5	740	0.33778	0.1877	0.80524	0.57027
10	424	494.26	499.3	738	0.29434	0.16571	0.83517	0.57453
12	422	479	484	724	0.2375	0.13507	0.67536	0.58287

From the values of these parameters the composition with X=4 shows best glass stability showing higher H_r and S parameter. The variation in glass transition temperature T_g can be explained on the basis of difference in the bond energies of Se and Te with Sn and Sb. The steep drop in the T_g in X=2 sample might be due to formation of weaker Te-Te bonds (bond energy 291.6 KJ/mole) since Sn and Sb favour strong bonds with Se (bond energy 401.2 and 346 kJ/mole respectively). On further substitution of Te, the reletively strong Sn-Te and Sb-Te bonds (bond energy 359.8 and 277.4 kJ/mole respectively) are formed leading to increase in the T_g. The decrease in T_g on further substitution of Te might be again formation of weaker Te-Te bonds due to abundance of Te in the X=12 Sample.

4. Conclusions

The thermal investigation of the chalcogenide system $Sn_{10}Sb_{20}Se_{70-X}Te_X$ was carried out. The variation of glass transition, crystallization temperature was evaluated from DSC plots. Glass transition temperature shows an increase upto X= 10 and then decreases. Apparent activation energy for glass transition and activation energy for crystallization were calculated using different theories. The crystallization kinetics showed volume nucleation and three-dimensional growth of cyrsallites. Thermal stability parameters were evaluated which showed the alloy with X=4 is the glass with best stability.

Acknowledgement

Author wants to thank Dr S. Sathiaraj of Botswana University and SAIF, Punjab University Chandigarh for XRD experiments and CIL, NIPER Mohali for their cooperation in conducting DSC Runs.

References

[1] A. Onozuka, O. Oda, J. Non-Cryst Solids **103,** 289 (1988).
[2] S.R. Elliot, Physics of amorphous materials, Longman publication, London (1991).
[3] S Fugimori, S Sagi, H Yamzaki, N Funakoski, J Appl. Phys. **64**, 100 (1988).

[4] T. Katsuyama, S. Satoh, H. Matsumura, J Appl. Phys. **71**, 4132 (1992).
[5] M. Asobe, OPTICAL FIBER TECHNOLOGY **3,** 142 (1997).
[6] E.R. Shaaban, M.T. Dessouky, A.M. Abousehly, j. Phys.: condens. Matter **19**, 096212 (2007).
[7] N. Afify, J. Non-Cryst. Solids **142**, 247 (1992).
[8] J. S. Sanghera, I.D. Aggarwal, J. Non-Cryst Solids **256&257**, 6 (1999).
[9] A.H. Moharram, A.A. Abu-sehly, M. Abu El-Oyoun, A.S. Soltan, Physica B **324,** 344 (2002).
[10] P. Kumar, R. Thanagraj, J. Non-Cryst Solids **352**, 2288 (2006).
[11] A.S. Soltan, Physica B **307**, 78 (2001).
[12] M Lasocka, Mater Sci Eng **23**, 173 (1976).
[13] H. E. Kissinger, J Res Nat. Bur. Stand. **57**, 217 (1956).
[14] D.R. Macfarlane, M. Matecki, M. poulain, J. Non-Cryst Solids **64**, 351 (1984).
[15] K. Matusita, T. Konatsu, R. Yokota, J. Mater. Sci. **19**, 291 (1984).
[16] S. Mahadevan, A Giridhar, A.K. Singh, J. Non-Cryst Solids **88**, 11 (1986).
[17] J. Colemenero, J.M. Bandarian, J. Non-Cryst Solids **30**, 263 (1978).
[18] A Dietzel, Glasstech. Ber. **22**, 41 (1968).
[19] A Hruby, Czech J Phys B **22,** 1187 (1972).
[20] M Saad, M Poulain, Mater. Sci. Forum **19/20,** 11 (1987).
[21] S Sakka, J.D Mackenzie, J. Non-Cryst Solids **6**, 145 (1971).
[22] K. Matusita, S. Sakka, Phys. Chem. Glasses **20**, 81 (1979).